HHS Public Access

Author manuscript

Nat Neurosci. Author manuscript; available in PMC 2012 August 13.

Published in final edited form as:

Nat Neurosci. 2011 June ; 14(6): 744–749. doi:10.1038/nn.2832.

The SK2-Long Isoform Directs Synaptic Localization and Function of SK2-containing channels

Duane Allen[1,+], **Chris T. Bond**[1,+], **Raphael Luján**[2,+], **Carmen Ballesteros-Merino**[2], **Mike T. Lin**[1], **Kang Wang**[1], **Nathan Klett**[1], **Masahiko Watanabe**[3], **Ryuichi Shigemoto**[4], **Robert W. Stackman**[5], **James Maylie**[6,*], and **John P. Adelman**[1,*]

[1]Vollum Institute, Oregon Health & Science University, Portland, Oregon 97239, USA

[2]Dept. Ciencias Médicas, Instituto de Investigación en Discapacidades Neurológicas (IDINE), Facultad de Medicina, Universidad Castilla-La Mancha, Campus Biosanitario, C/ Almansa 14, 02006 Albacete, Spain

[3]Department of Anatomy, Hokkaido University School of Medicine, Sapporo 060-8638, Japan

[4]Division of Cerebral Structure, National Institute for Physiological Sciences, Okazaki 444-8787, Japan

[5]Department of Psychology, and FAU/Max Planck Florida Institute Integrative Biology and Neuroscience Program, Florida Atlantic University, Boca Raton, FL 33431-0991, USA

[6]Department of Obstetrics and Gynecology, Oregon Health & Science University, Portland Oregon 97239, USA

Abstract

SK2-containing channels are expressed in the postsynaptic density (PSD) of dendritic spines on mouse CA1 pyramidal neurons, and influence synaptic responses, plasticity, and learning. The *SK2* gene encodes two isoforms differing only in the length of the N-terminal domain. SK2-Long (SK2-L) and SK2-Short (SK2-S) are co-expressed in CA1 pyramidal neurons and likely form heteromeric channels. In mice lacking SK2-L (*SK2-Sonly* mice), SK2-S-containing channels were expressed in the extrasynaptic membrane, but were excluded from the PSD. The SK channel contribution to EPSPs was absent in *SK2-Sonly* mice, and was restored by SK2-L re-expression. In slices from wild type mice, blocking SK channels increased the amount of long-term potentiation (LTP) induced in area CA1 but was without effect in *SK2-Sonly* mice. Further, *SK2-Sonly* mice outperformed wild type mice in the novel object recognition task. These results show that SK2-L directs synaptic SK2-containing channel expression, important for normal synaptic signaling, plasticity, and learning.

[*]Please address correspondences to Dr. James Maylie (mayliej@ohsu.edu) or Dr. John Adelman (adelman@ohsu.edu).
[+]These authors were equal contributors to this work.

AUTHOR CONTRIBUTIONS

D.A., M.T.L., K.W., and N.K. performed the electrophysiology, C.T.B. performed molecular biology and biochemistry, R.L., C.B-M. and R.S., were responsible for iEM, M.W. provided the antibodies, R.W.S. was responsible for the behavioural testing, J.M. and J.P.A. are corresponding authors.

INTRODUCTION

Dendritic spines are specialized compartments that form the postsynaptic sites for excitatory neurotransmission. Within the spine there are at least two anatomical and functional subdomains, the extrasynaptic membrane and the PSD, both of which contain α-amino-3-hydroxyl-5-methyl-4-isoxazole-propionate receptors (AMPARs) and N-Methyl-D-aspartic acid receptors (NMDARs)[1,2]. Proper and dynamic partitioning of AMPARs and NMDARs between the synaptic and extrasynaptic membranes is essential for normal neurotransmission[3–5], and at many synapses, such as the Schaffer collateral to CA1 synapses in the hippocampus, changes in the number and subunit composition of AMPARs and NMDARs in the PSD contribute to the expression of synaptic plasticity[6–9].

SK channels are activated solely by intracellular Ca^{2+} ions and selectively blocked by apamin[10]. SK2-containing channels are expressed in the PSD of dendritic spines on CA1 pyramidal neurons[11]. Spine SK2-containing channels are activated by synaptically driven Ca^{2+} influx and provide a repolarization that reduces the excitatory post-synaptic potential (EPSP), favoring Mg^{2+} re-block of NMDARs, and reducing the spine Ca^{2+} transient that is crucial to the induction of synaptic plasticity[11–13]. Indeed, field potential recordings in area CA1 show that blocking SK channels facilitates the induction of synaptic plasticity, and administration of apamin to mice facilitates hippocampus-dependent memory encoding[14]. Moreover, transgenic over-expression of SK2 impairs the induction of synaptic plasticity and severely impairs hippocampus-dependent memory encoding[15,16]. Similarly, administration of the SK channel agonist *N*-Cyclohexyl-*N*-[2-(3,5-dimethyl-pyrazol-1-yl)-6-methyl-4-pyrimidinamine (CyPPA) impairs the encoding of hippocampus-dependent object memory[17]. In addition, protein kinase A-dependent endocytosis of synaptic SK2 contributes to the expression of LTP[11,18]. Therefore, the expression of SK2-containing channels in the PSD is important for synaptic signaling, plasticity, and learning.

The *SK2* gene (*Kcnn2*) directs expression of two isoforms that differ only in the length of the intracellular N-terminal domain, with SK2-L having a 207 amino acid N-terminal extension compared to SK2-S. The two isoforms are expressed in many of the same brain regions, including hippocampus. SK2-L and SK2-S co-immunoprecipitate from brain, and when co-expressed heterologously, suggesting that they co-assemble into heteromeric channels[19]. When expressed separately, SK2-S and SK2-L form functional homomeric SK channels with similar Ca^{2+} sensitivity. Interestingly, homomeric SK2-S channels and homomeric SK2-L channels yield whole-cell currents of similar amplitude, but SK2-L currents in excised patches are much smaller than SK2-S currents. The inconsistency between whole-cell and patch current amplitudes for SK2-L reflects the strikingly punctate surface expression of SK2-L compared to the more uniform expression of SK2-S[19]. These results suggest that SK2-L may play a role in the subcellular localization of native SK2-containing channels. Therefore to investigate the roles of SK2-L in CA1 pyramidal neurons, we engineered mice that selectively lack the SK2-L isoform.

RESULTS

SK2-L is expressed in the PSD of CA1 pyramidal neurons

SK2-L is expressed in the dendrites in the *stratum radiatum*[19]. To determine the subcellular distribution of SK2-L, immunogold electron microscopy (iEM) was performed on hippocampal sections with an antibody directed against an epitope within the unique intracellular N-terminal domain (Supplementary Fig. S1). Pre-embedding immunogold labeling, to examine the extrasynaptic localization of SK2-L, showed that SK2-L was expressed in the plasma membrane of dendritic shafts and spines (Fig. 1a). Post-embedding immunogold labeling, to detect synaptic expression, showed that SK2-L was expressed in the PSD (Fig. 1b). From 50 spines with a total of 133 gold particles, 29% (38) were in the extrasynaptic spine membrane and 71% (95) were in the PSD. This result was verified using double immunogold labeling SDS-digested freeze-fracture replica (SDS-FRL) iEM for SK2-L, together with PSD-95 to delineate the synaptic membrane. SDS-FRL visualizes the two-dimensional distribution of membrane proteins with resolution and sensitivity beyond thin-section EM. The SK2-L antibody is directed against an intracellular epitope, so SK2-L was detected at the protoplasmic face (P-face) of the spine plasma membrane, consistent with the results of pre- and post-embedding experiments. Double immunolabeling for SK2-L and PSD-95 revealed co-clustering of the immunoparticles in spines, demonstrating SK2-L expression in the membrane at the PSD (Fig. 1c, see Fig. 3c).

SK2 is absent from the PSD in SK2-Sonly CA1 neurons

To investigate the physiological roles of the SK2-L isoform, transgenic mice selectively lacking SK2-L expression were generated. We have previously reported two different SK2 transgenic alleles. One is a *Cre-lox conditional* allele (Fig. 2a) that was used to make $SK2^{-/-}$ mice[20]. The other allele contains a *tetracycline regulated gene switch*[21] that was inserted in a position 5' to the translational initiator codon for SK2-S, but within the extended N-terminal coding sequence for SK2-L (*T* allele; Fig. 2b)[15]. To obtain mice selectively lacking SK2-L expression, $SK2^{+/T}$ mice were crossed with $SK2^{-/+}$ mice and $SK2^{-/T}$ (*SK2-Sonly*) mice were identified. In *SK2-Sonly* mice, neither SK2 isoform is expressed from the null allele, SK2-L is not expressed from the *T* allele, and SK2-S is over-expressed from the *T* allele[15]. Western blot analysis of brain proteins confirmed that *SK2-Sonly* mice lacked expression of SK2-L while SK2-S was over-expressed ~4-fold (Fig. 2c; Supplementary Fig. S2).

To determine the distribution of SK2 in spines in the presence and absence of SK2-L, post-embedding iEM was performed with a pan-SK2 antibody directed to the intracellular C-terminal domain[11]. In wild type spines SK2 was expressed in the extrasynaptic and synaptic membranes. From 71 spines with a total of 278 gold particles, 47% (130) were extrasynaptic and 53% (140) were at the PSD (Fig. 3a). In contrast, in *SK2-Sonly* mice, SK2-S was expressed in the extrasynaptic plasma membrane of dendritic spines, however, SK2-S was virtually absent from the PSD. From 82 spines with a total of 167 gold particles for SK2-S, 98% (164) were in the extrasynaptic spine membrane while 2% (3) of gold particles were at the PSD (Fig. 3b).

These results were confirmed and extended using SDS-FRL iEM. In contrast to the intermingled gold particles for PSD-95 and SK2-L (Fig. 1c) or PSD-95 and pan SK2-S (Fig. 3c) in wild type spines, replicas from *SK2-Sonly* mice that were double labeled for PSD-95 and for SK2 showed a segregation of the two populations of immunoparticles (Fig. 3d). The SDS-FRL results were quantified by measuring the distance from each SK2 gold particle to the nearest PSD-95 gold particle (Fig. 3e). Therefore, in the absence of SK2-L expression, SK2-S-containing channels were excluded from the PSD.

Synaptic SK2-containing channel function requires SK2-L

These results suggest that SK2 synaptic function would be lost in the absence of SK2-L expression. To first determine whether SK2-S-containing channels are functionally expressed in the absence of SK2-L, we used somatic step depolarizations in whole cell voltage clamp that activate an apamin sensitive SK current in wild type CA1 pyramidal neurons[14,20,22]. Following a depolarizing step to 20 mV to elicit an unclamped Ca^{2+} current, repolarizing the membrane to −55 mV evoked tail currents that were partially reduced by apamin (100 nM). Subtracting the traces recorded before and after apamin application yielded an apamin-sensitive current, I_{SK} (Fig. 4a). The apamin sensitive tail current measured 100 ms after repolarization in *SK2-Sonly* (357 ± 127 pA, n = 7) was larger than the apamin-sensitive current recorded from wild type littermates (95 ± 15 pA, n = 21; $P < 0.05$), reflecting SK2-S over-expression from the *T* allele in *SK2-Sonly* mice. To determine whether expression of SK2-L contributes further to the SK tail current, SK2-L was re-expressed in area CA1 of *SK2-Sonly* mice by transcranial delivery of a recombinant adeno-associated virus (rAAV) directing separate expression of SK2-L and GFP (Fig. 4b). Apamin-sensitive tail currents were recorded from *SK2-Sonly* non-fluorescent (*SK2-Sonly* inj. ctrl.) cells or fluorescent (*SK2-Sonly* inj. green) cells as well as CA1 pyramidal neurons from wild type littermates. The apamin-sensitive current was larger for *SK2-Sonly* injected cells, either crtl. or green, compared to wild type ($P < 0.05$), reflecting SK2-S over-expression. However, the apamin sensitive tail currents were not different compared to *SK2-Sonly* non-injected cells, and were not different between *SK2-Sonly* inj. ctrl. cells and *SK2-Sonly* inj. green cells (*SK2-Sonly* inj. ctrl: 293 ± 106 pA, n = 10; *SK2-Sonly* inj. green: 300 ± 68 pA, n = 11; Fig. 4c). Thus, re-expression of SK2-L in *SK2-Sonly* mice did not increase SK tail current amplitudes. These data extend our previous finding that SK2 expression is necessary for the apamin sensitive tail current in CA1 pyramidal neurons[20] and show that SK2-S-containing channels were sufficient for its expression.

To determine whether SK2 synaptic function is lost in the absence of SK2-L expression, synaptically evoked EPSPs were recorded from CA1 pyramidal neurons, before and after apamin application in brain slices prepared from rAAV-injected *SK2-Sonly* mice or wild type littermates. EPSPs were evoked every 30 sec by stimulation of Schaffer collateral axons. Following 10 min of stable baseline recordings, apamin (100 nM) was added and the EPSP amplitude was measured after 18–20 min. Apamin increased EPSPs in CA1 pyramidal neurons from wild type mice by 58 ± 12% (n = 8) as previously reported[12]. In contrast, apamin did not affect EPSPs recorded from *SK2-Sonly* inj. ctrl. CA1 pyramidal neurons (5 ± 6%, n = 10; Fig. 5a,b). However, apamin increased EPSPs from *SK2-Sonly* inj. green CA1 pyramidal neurons to the same extent as in wild type CA1 pyramidal neurons (44 ± 14%; n

= 10; Fig. 5a,b). These results show that SK2-L was necessary for SK channel synaptic function in CA1 pyramidal neurons.

SK channel activity does not affect LTP in SK2-Sonly mice

Apamin application to brain slices from wild type mice facilitates the induction of synaptic plasticity in area CA1 in response to conditioning stimulations of the Schaffer collateral axons[14]. To determine whether apamin altered LTP in the absence of synaptic SK2-containing channels, theta burst stimulation (TBS) was delivered to the Schaffer collateral axons with or without apamin application (100 nM) in hippocampal slices prepared from wild type and *SK2-Sonly* mice.

For wild type slices in control bath solution, TBS induced LTP, increasing the slope of the field EPSP (fEPSP) by 34 ± 4% (n = 12; $P < 0.05$). For wild type slices in apamin, TBS-induced LTP was enhanced, increasing the fEPSP slope by 59 ± 4% (n = 7; $P < 0.05$; Fig. 6a). In *SK2-Sonly* slices TBS also induced LTP to the same extent as in wild type slices, increasing the fEPSP by 40 ± 3% (n = 8) but this was not different than the LTP induced in the presence of apamin (47 ± 3%, n = 7; Fig. 6b,c). Therefore, the effects of apamin on LTP seen for wild type were absent in *SK2-Sonly* mice.

Altered memory encoding in SK2-Sonly mice

Systemic apamin administration facilitates the encoding of object memory[14]. To test whether this is a consequence of blocking synaptic SK2-containing channels, novel object recognition memory was examined in a naïve cohort of *SK2-Sonly* and wild type littermate mice. The mice (n = 13/group) were habituated to a novel high-walled arena for 10 min/day during Day 1 and 2. Locomotor responding declined over the course of habituation in both groups. However, the *SK2-Sonly* mice exhibited higher levels of locomotor behavior. There was an effect of genotype on distance measures ($P < 0.001$) and a significant genotype × min interaction ($P < 0.009$; Supplementary Fig. S3). On Day 3 each mouse was returned to the arena now containing two identical novel objects (the Sample Session). Mice were removed from the arena after achieving 19 sec of sample object exploration[14]. Wild type and *SK2-Sonly* mice exhibited equivalent latencies to reach criterion, indicating no difference in the motivation to explore objects during the Sample Session (Supplementary Fig. S4). For the Test Session (Day 4) each mouse was returned to the arena containing one familiar object and one novel object. The *SK2-Sonly* mice exhibited a significantly greater preference for exploring the novel object during the test session compared to the wild type mice ($P < 0.005$; Supplementary Fig. S4). These data indicate that the absence of synaptic SK2-containing channels was associated with a robust enhancement of non-spatial memory. This is similar to the effects of systemic apamin administration in wild type mice[14].

The same cohorts of mice received 24 training trials (4/day) in the hidden platform Morris water maze task. One *SK2-Sonly* mouse died before the start of water maze training. Over the course of training, *SK2-Sonly* mice (n = 12) exhibited poor spatial performance compared to wild type mice (n = 13; Fig. 7a). The slopes of the acquisition curves were similar for wild type and *SK2-Sonly* mice, indicating similar rates of spatial learning. However, the *SK2-Sonly* mice had longer latencies to find the submerged platform; there

was an effect of genotype ($P < 0.002$), and a genotype × trial block interaction ($P < 0.005$). *SK2-Sonly* mice also displayed poor retention of the platform location during 30 sec platform-less probe tests imposed after the 4th, 12th, and 20th training trials ($P < 0.003$; Fig. 7b). The paths taken during the probe test after the 20th training trial indicate that wild type mice (Fig. 7c, left) were arriving at the platform location by a direct path from the release point, and provide evidence of constrained search in the appropriate location of the maze. The paths taken by *SK2-Sonly* mice (Fig. 7c, right) were more circuitous and there was little evidence of appropriate search behavior. The mean percent dwell in the training quadrant during the last probe test for the wild type and *SK2-Sonly* groups were 34.8 ± 2.8% and 22.4 ± 3.9%, respectively ($P < 0.05$). The wild type and *SK2-Sonly* mice exhibited essentially equivalent learning in the visible platform version of the water maze. There was an effect of genotype on distance measures ($P < 0.001$) but a non-significant genotype × trial block interaction, ($P > 0.05$; Supplementary Fig. S5), suggesting that genotypic differences in sensorimotor function fail to explain the difference in spatial memory in the hidden platform task. The behavior of the *SK2-Sonly* mice in the Morris water maze task was distinct from wild type mice. The *SK2-Sonly* mice did not develop a spatial bias in their search for the platform and would often swim over the platform or fail to remain on the platform after finding it. Thus, the impairment in this task may reflect motivational or attention deficits that influence performance in the Morris water maze. These data indicate that the absence of SK2-L was associated with an impairment of spatial learning and memory in the Morris water maze.

DISCUSSION

The results show that the SK2-L isoform directed synaptic localization of SK2-containing channels that is necessary for their synaptic functions, including modulation of EPSPs and synaptic plasticity. Consistent with these synaptic roles, the SK2-L isoform was required for normal hippocampus-dependent learning. In the absence of SK2-L, SK2-S-containing channels were expressed on the extrasynaptic plasma membrane o f dendritic spines but they were selectively excluded from the PSD.

Northern blot analysis for SK2 mRNA detects a doublet of 2.2 and 2.4 kilobases[10]. However, these mRNA sizes are not sufficient to encode SK2-L, suggesting that SK2-S and SK2-L are translated from different mRNAs, and that the SK2-L mRNA is in low steady state abundance and may be rapidly turned over. The SK2-S mRNA CAP site (unpublished result) and the SK2-S promoter[23] are localized within the SK2-L transcript. Mapping the 5' untranslated sequences in the SK2-L mRNA onto the *SK2* gene showed that the promoter responsible for expression of the SK2-L mRNA must reside ~300 kilobase pairs 5' of the promoter for SK2-S mRNA[23]. Thus, it appears that the SK2-L and SK2-S mRNAs are transcribed from independent promoters (see Fig. 2). Indeed, 50–60% of human and mouse genes may use alternative promoters[24] that many times result in expression of distinct protein isoforms. The SK2-L transcript is conserved between mouse and human, and a cDNA from human hippocampus encoding the extended amino terminus of SK2-L has been identified (human EST DB636479.1) suggesting that the two SK2 isoforms, the molecular mechanisms that generate them, and their roles in synaptic localization and function, are conserved.

In mice lacking SK2-L, synaptic SK2-S-containing channels were absent. This could mean that in wild type CA1 pyramidal neurons synaptic SK2-containing channels are homomeric assemblies of SK2-L. The SK2-L antibody demonstrated that SK2-L was expressed in the PSD of wild type CA1 pyramidal neurons, but because the SK2-S amino acid sequence is completely contained in SK2-L we could not generate an SK2-S specific antibody to independently examine SK2-S for synaptic expression. However, SK2-L and SK2-S subunits co-immunoprecipitate from brain, strongly suggesting that they form heteromeric channels[19]. In $SK2^{+/T}$ mice that over-express SK2-S in the presence of SK2-L, apamin increases EPSPs more than in wild type mice[15], suggesting that the excess SK2-S subunits contribute to synaptic SK2-containing channels. Therefore, it is likely that synaptic SK2-containing channels are heteromeric assemblies of SK2-L and SK2-S subunits and that at least one SK2-L subunit is required for synaptic expression. Whether SK2-L is sufficient for synaptic expression and function awaits experiments in mice that express only SK2-L. The SK1 and SK3 mRNAs are also expressed in CA1 pyramidal neurons[25], and SK3 also co-immunoprecipitates with SK2-L from brain[19]. The SK3 N-terminal domain is similar in length to SK2-L and contains several regions of homology. The functions of SK1 and SK3 in CA1 pyramidal neurons remain unknown. However, the lack of apamin sensitivity to EPSPs in *SK2-Sonly* CA1 pyramidal neurons suggests that SK2-L was necessary for synaptic function and that SK3 cannot substitute for SK2-L.

Recordings from CA1 pyramidal neurons demonstrated that in the absence of SK2-L, synaptic SK channel activity was absent, and was re-instated by re-expression of SK2-L. However, SK2-L re-expression did not increase the amplitude of apamin-sensitive tail currents in *SK2-Sonly* CA1 pyramidal neurons, suggesting that SK2-L may not increase surface expression per se, but may direct selective synaptic localization. Further, in response to TBS apamin increased LTP in brain slices from wild type, but not *SK2-Sonly* mice, suggesting that blocking synaptic SK channel activity with apamin is responsible for the increased LTP. Interestingly, the amount of LTP induced in slices from *SK2-Sonly* mice was not significantly different from the LTP induced in wild type slices in the absence of apamin. This may reflect the over-expression of non-synaptic SK2-S or compensatory changes in the *SK2-Sonly* mice.

Synaptic localization of SK2-containing channels is important for normal synaptic responses[12]. In contrast to glutamate receptors, SK2 does not contain a post-synaptic density protein, Drosophila disc large tumor suppressor, zonula occludens-1 protein (PDZ) ligand and therefore must employ a distinct molecular strategy for synaptic localization. Interestingly, recent results demonstrate that a Ca^{2+}-calmodulin kinase II phosphorylation site in the first intracellular loop of the GluA1 subunit is critical for receptor targeting to synapses, but not for delivery of GluA1-containing AMPARs to the plasma membrane[26]. This PDZ-independent effect on trafficking of GluA1-containing AMPARs selectively to the synaptic membrane is similar to the synaptic localization endowed by the SK2-L subunit.

Previous studies have shown that SK channel activity affects learning and memory[14–16]. In the non-spatial object recognition task the *SK2-Sonly* mice phenocopied wild type mice treated with apamin, showing improved memory encoding. This demonstrated that SK2-L

expression was required for normal performance in the object recognition task, and suggests that apamin and SK2-L deficiency both mediate their effects on object recognition through the loss of synaptic SK2-containing channel function. In contrast, *SK2-Sonly* mice were impaired in the spatial learning Morris water maze task, different than the facilitation in this task seen with apamin administration[14]. This might reflect compensatory alterations that are not observed with acute channel block by apamin. The Morris water maze task requires several trials presented over several days and it is also possible that experience-dependent endocytosis and subsequent repopulation of synaptic SK2-containing channels are necessary for normal acquisition of the Morris water maze task. Notably, transgenic SK2 over-expression also results in impaired performance in the Morris water maze task[15], and in both of these transgenic models, there are increased apamin sensitive tail currents that might, in part, reflect dendritic SK2-containing channel activity. These channels may alter synaptic integration and could contribute to the deficits in water maze performance. Taken together, the anatomical, electrophysiological, and behavioral results from both tasks demonstrate that SK2-L expression was essential for normal synaptic responses, plasticity, and learning.

METHODS

Animal care

All procedures were performed in accordance with the guidelines of the Oregon Health & Science University, the University of Castilla-La Mancha, and Florida Atlantic University, and the Animal Care and Use Committee of the respective institutions approved all experimental procedures.

Antibodies

Two affinity-purified polyclonal antibodies against SK2 were raised in rabbit and guinea pig, respectively. The specificity of the guinea pig pan-SK2 antibody has been previously described elsewhere[11]. The mouse monoclonal antibody against PSD-95 was obtained from Abcam.

Immuno electron microscopy

Immunohistochemical reactions for pre- and post-embedding EM were performed as previously described[27]. Ultrastructural analyses were performed in a Jeol-1010 electron microscope.

Pre-embedding immunogold

Briefly, free-floating sections were incubated in 10% NGS (Normal Goat Serum) diluted in Tris-buffered saline (TBS) for 1 hour at room temperature. Sections were then incubated for 48 hours in anti-pan SK2 or anti-SK2-L antibodies (1–2 μg/ml) diluted in 1% NGS (normal goat serum)/TBS. After washes in TBS, sections were incubated for 3 hours in goat anti-rabbit IgG or goat anti-guinea pig IgG coupled to colloidal gold particles (Nanoprobes Inc.) diluted 1:100 in 1% NGS/TBS. After washes in phosphate-buffered saline (PBS), the sections were postfixed in 1% glutaraldehyde diluted in the same buffer for 10 min, washed in double distilled water, followed by silver enhancement of the gold particles with a HQ Silver kit (Nanoprobes Inc.). Sections were then treated with osmium tetraoxide (1% in 0.1

M PB), block-stained with uranyl acetate, dehydrated in graded series of ethanol and flat-embedded on glass slides in Durcupan (Fluka) resin. Regions of interest were cut at 70–90 nm on an ultramicrotome (Reichert Ultracut E) and collected on 200-mesh nickel grids. Staining was performed on drops of 1% aqueous uranyl acetate followed by Reynolds's lead citrate.

Post-embedding immunogold

Ultrathin sections 80-nm thick from Lowicryl-embedded blocks of hippocampus were picked up on coated nickel grids and incubated for 45 min on drops of a blocking solution consisting of 2% Human Serum Albumin (HSA) in 0.05 M TBS and 0.03% Triton X-100 (TBST). The grids were incubated with pan-SK2 or SK2-L antibodies (10 μg/ml) in TBST with 2% HSA at 28 °C overnight. After washing, the grids were incubated for 3 h on drops of goat anti-guinea pig IgG or goat anti-guinea pig IgG conjugated to colloidal gold particles (Nanoprobes Inc.) diluted 1:80 in 2% HSA and 0.5% polyethylene glycol in TBST. The grids were then washed in TBS for 30 min and counterstained for EM with saturated aqueous uranyl acetate followed by lead citrate.

SDS-FRL

SDS-FRL was performed according to Fujimoto[28] with some modifications. Animals were anesthetized with sodium pentobarbital and subjected to transcardiac perfusion with formaldehyde (0.5%; freshly depolymerized from paraformaldehyde) in 0.1 M sodium phosphate buffer. After perfusion, brains were removed. The hippocampi were cut into sections 120 μm-thick using a Microslicer (Dosaka), and cryoprotected with 32% glycerol in PBS for 12–16 hours. The sections were then frozen by a high-pressure freezing machine (HPM 010; Bal-Tec), and fractured by the double replica method in a freeze etching system (BAF 060; Bal-Tec). The fractured faces were replicated by carbon (5 nm) with an electron beam gun from overhead and shadowed by platinum/carbon positioned at a 25° angle with rotating (2.5 nm) or at a 45° angle (2 nm) unidirectionally, followed by carbon (20 nm) applied from overhead. We applied 5 nm of carbon before platinum to increase the detection efficiency. The pieces of replica were transferred to 2.5% SDS containing 62.5 mM Tris and 10% glycerol, pH 6.8. SDS treatment was performed for 15 min at 105 °C with autoclaving, 16 hours at 80 °C with shaking, or 16 hours at 30 °C with vigorous stirring. After the treatment with SDS, replicas were washed with three changes of 0.1% BSA in TBS and blocked for 1 hour, with two changes of 5% BSA/TBS. The replicas were then reacted with a mixture of anti-pan SK2 or anti-SK2-L and monoclonal antibody for PSD-95 at room temperature for 1 hour, followed by 4 °C for 36–48 h. Following three washes in 0.1% BSA in TBS and blocking in 5% BSA/TBS, replicas were incubated in a mixture of secondary antibodies (goat anti-guinea pig IgG and goat anti-mouse IgG coupled to gold particles (British Biocell International) for 1 hour at room temperature, followed by 12–16 hours at 4 °C. When one of the primary antibodies was omitted, no immunoreactivity for the omitted primary antibody was observed. After immunogold labeling, the replicas were immediately rinsed three times with 0.1% BSA/TBS, washed twice with distilled water, and picked up onto grids coated with pioloform (Agar Scientific).

Western blots

Hippocampal membranes were prepared from adult wild type, *SK2-Sonly*, and *SK2*$^{-/-}$ mice as previously reported[19]. Forty micrograms of protein were separated by SDS-PAGE and transferred to nitrocellulose membranes. The membranes were probed with pan anti-SK2 (3 μg/ml) or with anti-SK2-L (1 μg/ml). Protein bands were visualized after application of anti-rabbit-HRP secondary antibody (Promega) at 1:20,000 using Supersignal West Pico Chemoluminescent ECL (Thermo Scientific).

Virus injections

Three to four week old animals were anesthetized with isoflurane, immobilized in a Kopf Stereotaxic Alignment System, and injected with 0.2 μl of virus solution (2×10^{10} vg/ml) at 2–6 sites targeting the hippocampus with the Quintessential Stereotaxic Injector (Stoelting). Recordings were performed more than 14 days after surgery.

Slice preparation

Hippocampal slices were prepared from 6–10-week-old C57BL/6J mice as previously described[11,12]. Slices were transferred into a holding chamber containing artificial cerebrospinal fluid (aCSF) (in mM): 125 NaCl, 2.5 KCl, 21.5 $NaHCO_3$, 1.25 NaH_2PO_4, 2.0 $CaCl_2$, 1.0 $MgCl_2$, 15 glucose and equilibrated with carbogen. Slices were incubated at 34 °C for 30 min and then at room temperature for ≥1 hour before recordings were performed.

Electrophysiology

Whole-cell patch-clamp recordings were obtained from CA1 pyramidal cells as previously described[11,12]. Patch pipettes (open pipette resistance, 2–4 MΩ) were filled with a solution containing (in mM): 130 K-gluconate, 8 NaCl, 1 $MgCl_2$, 10 HEPES, 4 ATP, 0.3 GTP, and 10 phosphocreatine, pH 7.26. In voltage clamp, series resistance was compensated to > 80%. For current clamp, series resistance was not electronically compensated and recordings with series resistance that changed more than 20% during the experiment were discarded. All recordings were from cells with a resting membrane potential between −70 and −50 mV, and a stable input resistance. A bias current was applied to maintain the membrane potential at −60 mV in current clamp. All whole cell recordings were performed at room temperature.

Field recordings

Extracellular field potentials (fEPSPs) were recorded as previously described[14,15]. LTP was induced by a theta-burst stimulation (TBS) protocol consisting of 10 theta bursts at 5 Hz; each theta burst contains 4–5 pulses at 100 Hz. The initial slope of the fEPSP was measured to monitor the strength of synaptic transmission, minimizing contamination by voltage-dependent events. Summary graphs were obtained by normalizing each experiment according to the average value of all points on the 10 min baseline. Field recordings were performed at 30–32 °C.

Synaptic stimulations

Capillary glass pipettes filled with aCSF, with a tip diameter of 1–2 μm, connected to Model 2200 stimulus isolation unit (whole cell recordings; A–M Systems) and a Digitimer DS3

stimulus isolation unit (field recordings; Automate Scientific). SR95531 (2 μM) and CGP55845 (1 μM) were present to reduce $GABA_A$ and $GABA_B$ contributions, respectively. To prevent epileptic discharges in the presence of GABAergic blockers, the CA3 region was microdissected out before recording.

Data analysis

Data were analyzed using IGOR (WaveMetrics). A non-parametric Wilcoxon-Mann-Whitney two-sample rank test or a paired two-sample *t*-test was used to determine significance of data; $P < 0.05$ was considered significant.

Chemicals

CGP55845, and SR95531 were obtained from Tocris Cookson. Apamin was from Calbiochem.

Behavioral Testing

All mice were acclimated to the laboratory prior to initiating behavioral testing.

Spontaneous Novel Object Recognition

As described previously[14], during the sample session each mouse explored two novel toy objects in the familiar white ABS arena (37.5 cm × 37.5 cm × 50.8 cm tall). Mice were removed from the arena after accumulating 19 sec of sample object exploration; any mice that failed to reach this encoding criterion within 10 min were removed from the study. During the test session 24 hours later, each mouse was returned to the arena for a 5-min session and the arena contained one of the objects from the sample session and a novel object. Object exploration was recorded with digital stopwatches for the sample session and with the Ethovision XT (Leesburg, VA) manual event encoder for the test session. Exploration was defined as time spent with the head oriented towards the object and within 2–3 cm. Measures were *Latency to accumulate sample object exploration*, defined as the amount of time (in seconds) each mouse took to reach the encoding criterion during the sample session; and *Novel object preference ratio*, defined as the time spent exploring the novel object divided by the total time spent exploring both test session objects.

Morris Water Maze

Mouse behavior was recorded with the EthoVision XT video-tracking system. As described previously[14], mice received 6 days of *hidden platform training* (4 trials/day), to learn the location of a clear Plexiglas platform (8 cm diameter) submerged 1 cm below the surface of the pool (60 cm high, 109 cm diameter). Large visible cues were present around the pool. Mice remained on the platform for 30 sec, and then were placed into a holding cage for a 45 sec inter-trial interval. To examine spatial memory retention, mice received a 30-s probe test 5 min after the 4^{th}, 12^{th} and 20^{th} training trial during which the platform was removed from the pool. *Percent dwell in each pool quadrant* was determined for each mouse and *search ratio* was calculated from probe test behavior as the number of crossings into a 23.8 cm diameter circular zone around the platform location, divided by the total number of crossings into four equivalent zones (in each of the four pool quadrants). During *visible*

platform training (6 trials/day), each mouse swam to a black Plexiglas platform (13 cm diameter) located just above the water's surface at a position that was randomized each trial.

Data analysis

The Morris water maze data were analyzed with two-factor, repeated measures (genotype, day or probe test) ANOVA with post-hoc Student's t-tests where appropriate. The novel object recognition data for latency to accumulate sample object exploration and the novel object preference ratio were analyzed with Student's t-tests. $P < 0.05$ was considered significant.

Supplementary Material

Refer to Web version on PubMed Central for supplementary material.

ACKNOWLEDGEMENTS

This work was supported by NIH grants NS038880 (JPA) and MH081860-01 (JM), F32MH080480 (MTL), and MH0876591-01 and NSF grant IBN 0630522 (RWS), and grants from the Spanish Ministry of Education and Science (CONSOLIDER CSD2008-00005), and from Consejería de Educación y Ciencia, Junta de Comunidades de Castilla-La Mancha (PAI08-0174-6967) to R.L. Special thanks is given to Kyle Vick, Christina Christakis and Kristine Smith (all from FSU) for their expert assistance with the behavioural testing.

LITERATURE CITED

1. Bredt DS, Nicoll RA. AMPA receptor trafficking at excitatory synapses. Neuron. 2003; 40:361–379. [PubMed: 14556714]
2. Petralia RS, Wenthold RJ. Light and electron immunocytochemical localization of AMPA-selective glutamate receptors in the rat brain. J Comp Neurol. 1992; 318:329–354. [PubMed: 1374769]
3. Carroll RC, Zukin RS. NMDA-receptor trafficking and targeting: implications for synaptic transmission and plasticity. Trends Neurosci. 2002; 25:571–577. [PubMed: 12392932]
4. Adesnik H, Nicoll RA, England PM. Photoinactivation of native AMPA receptors reveals their real-time trafficking. Neuron. 2005; 48:977–985. [PubMed: 16364901]
5. Harris AZ, Pettit DL. Recruiting extrasynaptic NMDA receptors augments synaptic signaling. J Neurophysiol. 2008; 99:524–533. [PubMed: 18057106]
6. Makino H, Malinow R. AMPA receptor incorporation into synapses during LTP: the role of lateral movement and exocytosis. Neuron. 2009; 64:381–390. [PubMed: 19914186]
7. Derkach VA, Oh MC, Guire ES, Soderling TR. Regulatory mechanisms of AMPA receptors in synaptic plasticity. Nat Rev Neurosci. 2007; 8:101–113. [PubMed: 17237803]
8. van Zundert B, Yoshii A, Constantine-Paton M. Receptor compartmentalization and trafficking at glutamate synapses: a developmental proposal. Trends Neurosci. 2004; 27:428–437. [PubMed: 15219743]
9. Bellone C, Nicoll RA. Rapid bidirectional switching of synaptic NMDA receptors. Neuron. 2007; 55:779–785. [PubMed: 17785184]
10. Köhler M, et al. Small-conductance, calcium-activated potassium channels from mammalian brain [see comments]. Science. 1996; 273:1709–1714. [PubMed: 8781233]
11. Lin MT, Lujan R, Watanabe M, Adelman JP, Maylie J. SK2 channel plasticity contributes to LTP at Schaffer collateral-CA1 synapses. Nat Neurosci. 2008; 11:170–177. [PubMed: 18204442]
12. Ngo-Anh TJ, et al. SK channels and NMDA receptors form a Ca2+-mediated feedback loop in dendritic spines. Nat Neurosci. 2005; 8:642–649. [PubMed: 15852011]
13. Bloodgood BL, Sabatini BL. Nonlinear regulation of unitary synaptic signals by CaV(2.3) voltage-sensitive calcium channels located in dendritic spines. Neuron. 2007; 53:249–260. [PubMed: 17224406]

14. Stackman RW, et al. Small conductance Ca2+-activated K+ channels modulate synaptic plasticity and memory encoding. J Neurosci. 2002; 22:10163–10171. [PubMed: 12451117]
15. Hammond RS, et al. Small-conductance Ca2+-activated K+ channel type 2 (SK2) modulates hippocampal learning, memory, and synaptic plasticity. J Neurosci. 2006; 26:1844–1853. [PubMed: 16467533]
16. Stackman RW Jr, Bond CT, Adelman JP. Contextual memory deficits observed in mice overexpressing small conductance Ca2+-activated K+ type 2 (KCa2.2, SK2) channels are caused by an encoding deficit. Learn Mem. 2008; 15:208–213. [PubMed: 18385475]
17. Vick, KAt; Guidi, M.; Stackman, RW, Jr. In vivo pharmacological manipulation of small conductance Ca(2+)-activated K(+) channels influences motor behavior, object memory and fear conditioning. Neuropharmacology. 2010; 58:650–659. [PubMed: 19944112]
18. Lin MT, et al. Coupled activity-dependent trafficking of synaptic SK2 channels and AMPA receptors. J Neurosci. 2010; 30:11726–11734. [PubMed: 20810893]
19. Strassmaier T, et al. A novel isoform of SK2 assembles with other SK subunits in mouse brain. J Biol Chem. 2005; 280:21231–21236. [PubMed: 15797870]
20. Bond CT, et al. Small conductance Ca2+-activated K+ channel knock-out mice reveal the identity of calcium-dependent afterhyperpolarization currents. J Neurosci. 2004; 24:5301–5306. [PubMed: 15190101]
21. Bond CT, et al. Respiration and parturition affected by conditional overexpression of the Ca2+-activated K+ channel subunit, SK3. Science. 2000; 289:1942–1946. [PubMed: 10988076]
22. Stocker M, Krause M, Pedarzani P. An apamin-sensitive Ca^{2+}-activated K^{+} current in hippocampal pyramidal neurons. Proc. Natl. Acad. Sci. USA. 1999; 96:4662–4667. [PubMed: 10200319]
23. Kye MJ, Spiess J, Blank T. Transcriptional regulation of intronic calcium-activated potassium channel SK2 promoters by nuclear factor-kappa B and glucocorticoids. Mol Cell Biochem. 2007; 300:9–17. [PubMed: 17396235]
24. Davuluri RV, Suzuki Y, Sugano S, Plass C, Huang TH. The functional consequences of alternative promoter use in mammalian genomes. Trends Genet. 2008; 24:167–177. [PubMed: 18329129]
25. Stocker M, Pedarzani P. Differential distribution of three Ca(2+)-activated K(+) channel subunits, SK1, SK2, and SK3, in the adult rat central nervous system. Mol Cell Neurosci. 2000; 15:476–493. [PubMed: 10833304]
26. Lu W, Isozaki K, Roche KW, Nicoll RA. Synaptic targeting of AMPA receptors is regulated by a CaMKII site in the first intracellular loop of GluA1. Proc Natl Acad Sci U S A. 2010
27. Lujan R, Nusser Z, Roberts JD, Shigemoto R, Somogyi P. Perisynaptic location of metabotropic glutamate receptors mGluR1 and mGluR5 on dendrites and dendritic spines in the rat hippocampus. Eur J Neurosci. 1996; 8:1488–1500. [PubMed: 8758956]
28. Fujimoto K. Freeze-fracture replica electron microscopy combined with SDS digestion for cytochemical labeling of integral membrane proteins. Application to the immunogold labeling of intercellular junctional complexes. J Cell Sci. 1995; 108(Pt 11):3443–3449. [PubMed: 8586656]

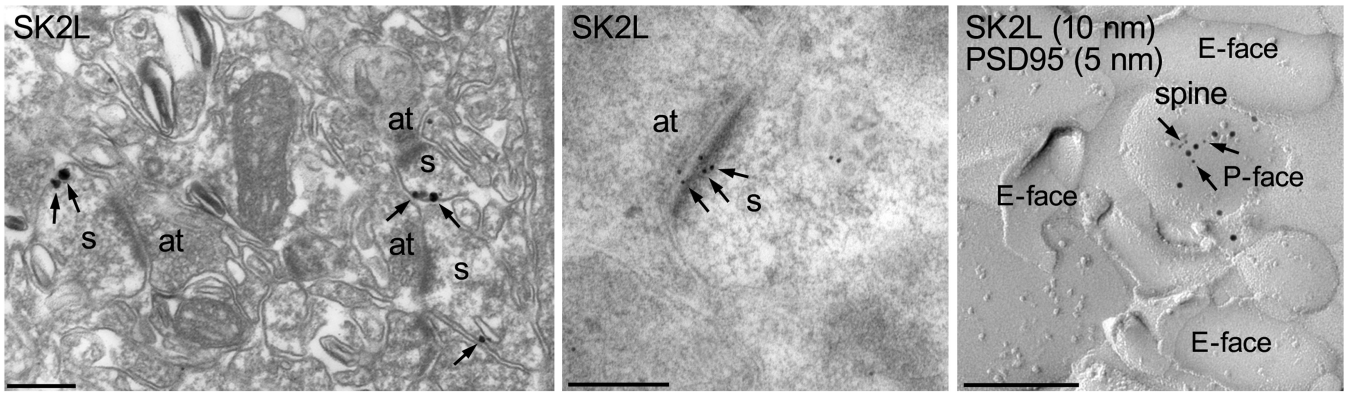

Figure 1. Subcellular localization of SK2-L in dendritic spines of wild type CA1 pyramidal neurons

(**a**) Using the pre-embedding technique, immunoparticles for SK2-L were detected along the extrasynaptic plasma membrane (arrows) of dendritic spines (s). (**b**) Using the post-embedding technique, immunoparticles for SK2-L were detected along the PSD (arrows) of dendritic spines (s). (**c**) Using the SDS-FRL technique, the synaptic membrane was identified by immunoparticles for PSD-95 (arrows). SK2-L immunoparticles were detected in dendritic spines intermingled with immunoparticles for PSD-95. at: axon terminal; scale bars: 200 nm.

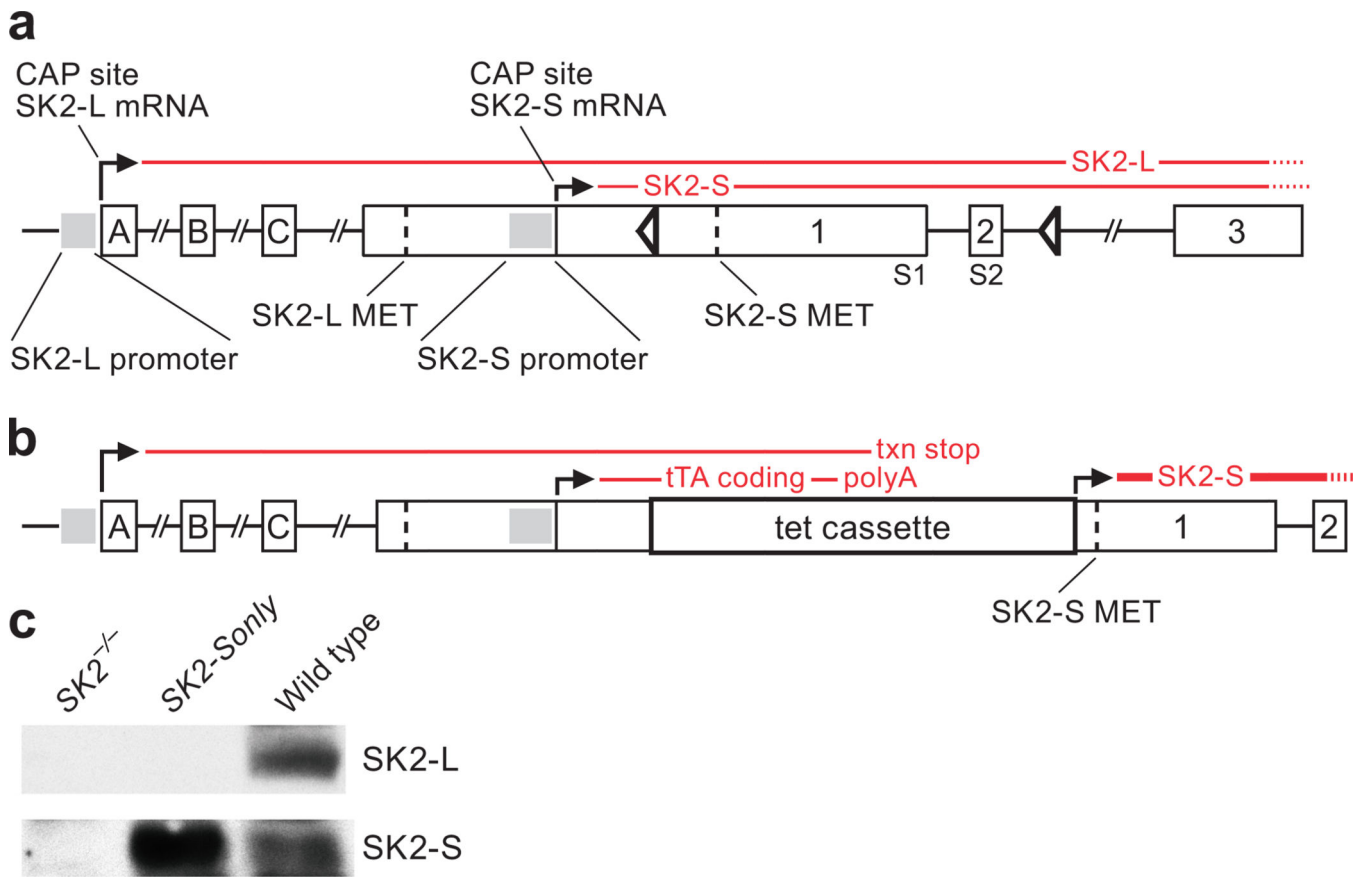

Figure 2. *SK2* gene locus and Western blot

(**a**) The 5’ region of the mouse *SK2* gene. Boxes represent exons. The positions of the translational initiator methionine (Met) codons for SK2-L and SK2-S are shown as dotted lines. The 5’ end of the longest SK2-L cDNA resides within exon A, while the CAP site for the SK2-S mRNA resides in exon 1. The shaded areas indicate positions of the promoters that drive SK2-L and SK2-S expression. The lines above the exon-intron mosaic indicate the transcripts for SK2-L and SK2-S. The triangles show the positions of the *LoxP* sites in the *floxed SK2* allele. (**b**) The mouse *SK2 T* allele. The position of the *tet gene switch* is indicated in the SK2-S 5’ untranslated region, 5’ of the SK2-S initiator Met. The SK2-L transcript is terminated within the inserted *tet cassette*, abolishing SK2-L expression. The SK2-S promoter drives expression of the tetracycline transactivator (tTA) mRNA. The tTA protein binds to *Tet operator* sequences at the 3’ end of the *tet cassette* and enables SK2-S over-expression from the *minimal CMV promoter*. (**c**) Western blots of hippocampal proteins probed for SK2 in wild type, *SK2-Sonly*, and $SK2^{-/-}$ mice using the SK2-L antibody (top blot) and the pan-SK2 antibody (bottom blot).

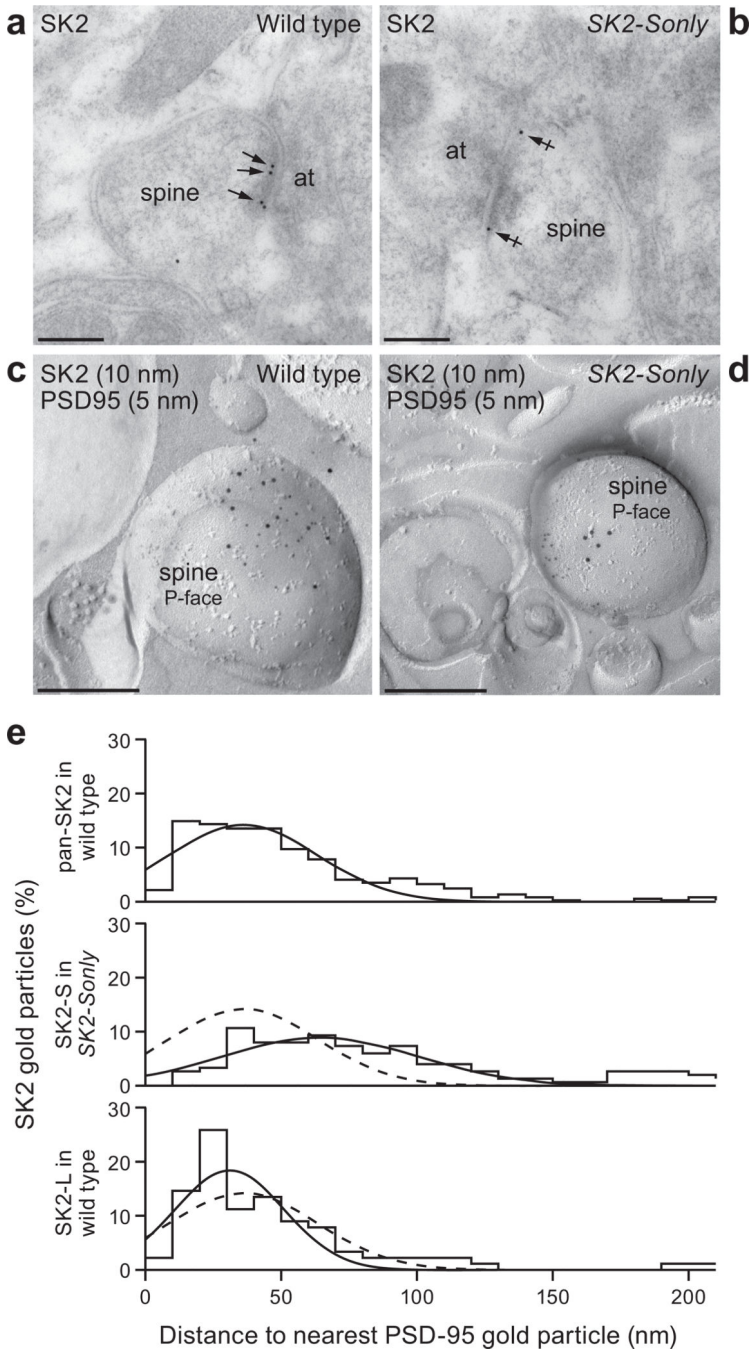

Figure 3. Subcellular localization of SK2 in wild type and *SK2-Sonly* CA1 pyramidal neurons

(**a**) Using the post-embedding technique in wild type, immunoparticles for SK2 were detected along the PSD (arrows) of dendritic spines. (**b**) Using the post-embedding technique in *SK2-Sonly*, immunoparticles for SK2 were detected along the extrasynaptic membrane (arrows) of dendritic spines but not along the PSD. (**c**) Using the SDS-FRL technique in wild type, SK2 immunoparticles were detected in dendritic spines intermingled with immunoparticles for PSD-95. (**d**) Using the SDS-FRL technique in *SK2-Sonly*, and double immunolabeling for SK2 and PSD-95, SK2 immunoparticles were detected in

dendritic spines but segregated from immunoparticles for PSD-95. Scale bars: 200 nm. (**e**) For SDS-FRL immunolabeling, the percentage of SK2 immunoparticles was plotted as a function of distance from the nearest PSD-95 immunoparticle, and fit by Gaussians for the indicated groups. Dashed line in middle and bottom panels is the fit from wild type in upper panel.

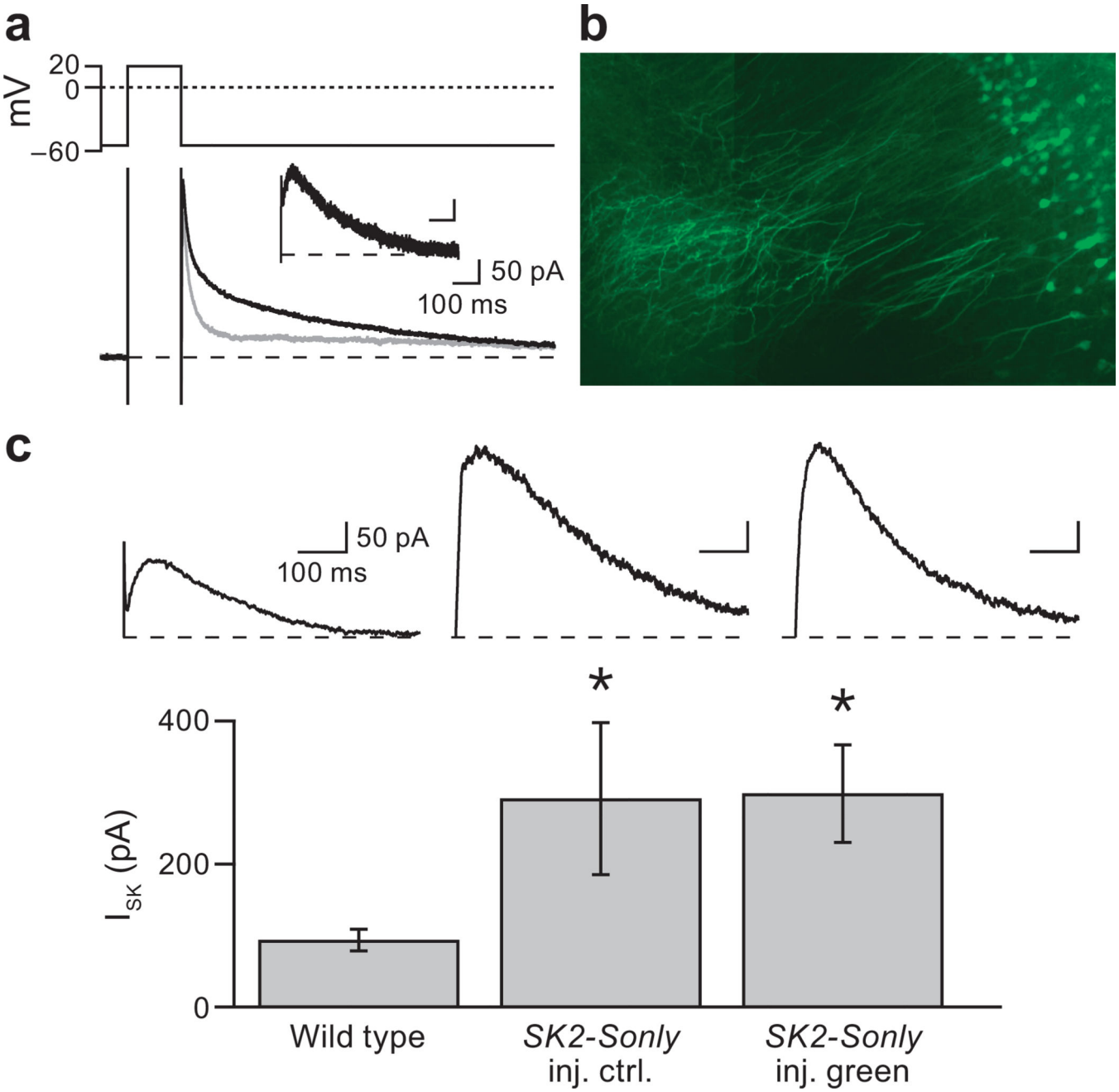

Figure 4. SK2-containing channels are expressed in the plasma membrane of *SK2-Sonly* CA1 pyramidal neurons

(a) top: Voltage protocol used to evoke tail currents. Cells were voltage clamped at −55 mV, and tail currents were elicited after 200 ms depolarizing steps to 20 mV; bottom: representative tail currents from a wild type CA1 neuron before (black trace) and after (grey trace) apamin application. The inset shows the subtracted apamin-sensitive current. (**b**) Section through hippocampus from an *SK2-Sonly* mouse injected with rAAV directing separate expression of GFP and SK2-L. (**c**) top: Representative apamin-sensitive currents from wild type (left), *SK2-Sonly* inj. ctrl. (middle), and *SK2-Sonly* inj. green (left) CA1

pyramidal neurons; bottom: Summary plot shows that the amplitude of apamin-sensitive currents (I_{SK}) for the three groups of neurons. Error bars indicate s.e.m. *P < 0.05 for wild type compared to *SK2-Sonly* inj. ctrl. or *SK2-Sonly* inj. green.

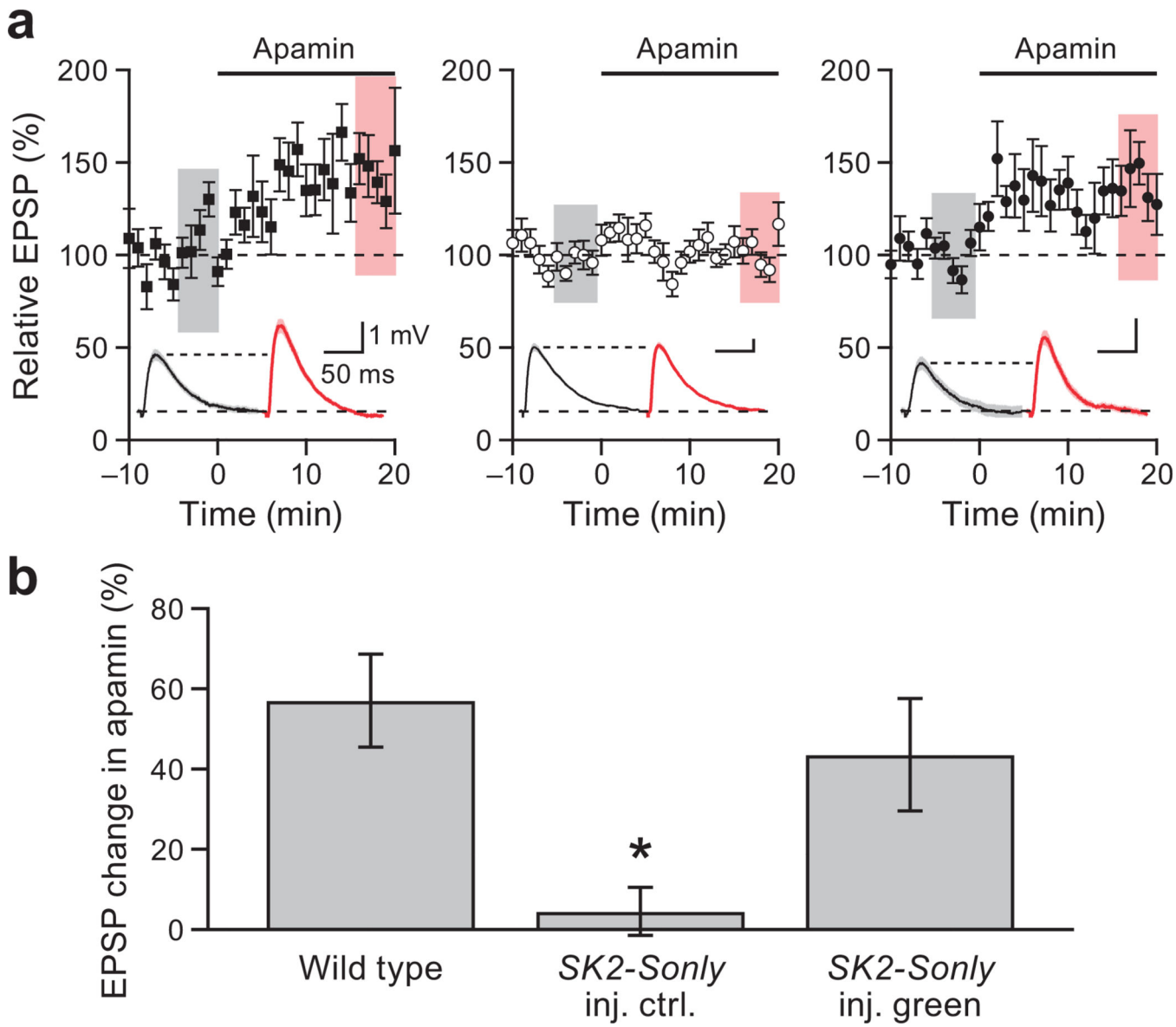

Figure 5. SK2-L re-expression re-instates apamin sensitivity to synaptically evoked glutamatergic EPSPs

(**a**) Time course of the normalized EPSP amplitude (mean ± s.e.m.) before and after apamin application for wild type (left), *SK2-Sonly* inj. ctrl. (middle), and *SK2-Sonly* inj. green (right) CA1 pyramidal neurons. Insets show representative average of 20 EPSPs, mean ± s.e.m. (shaded area), taken from the indicated shaded time points in control condition before (black line; left) and after (red line; right) apamin application. (**b**) Bar graph of the increase in EPSP following apamin application. Error bars indicate s.e.m. *P < 0.05 for *SK2-Sonly* inj. ctrl. and *SK2-Sonly* inj. green compared to wild type.

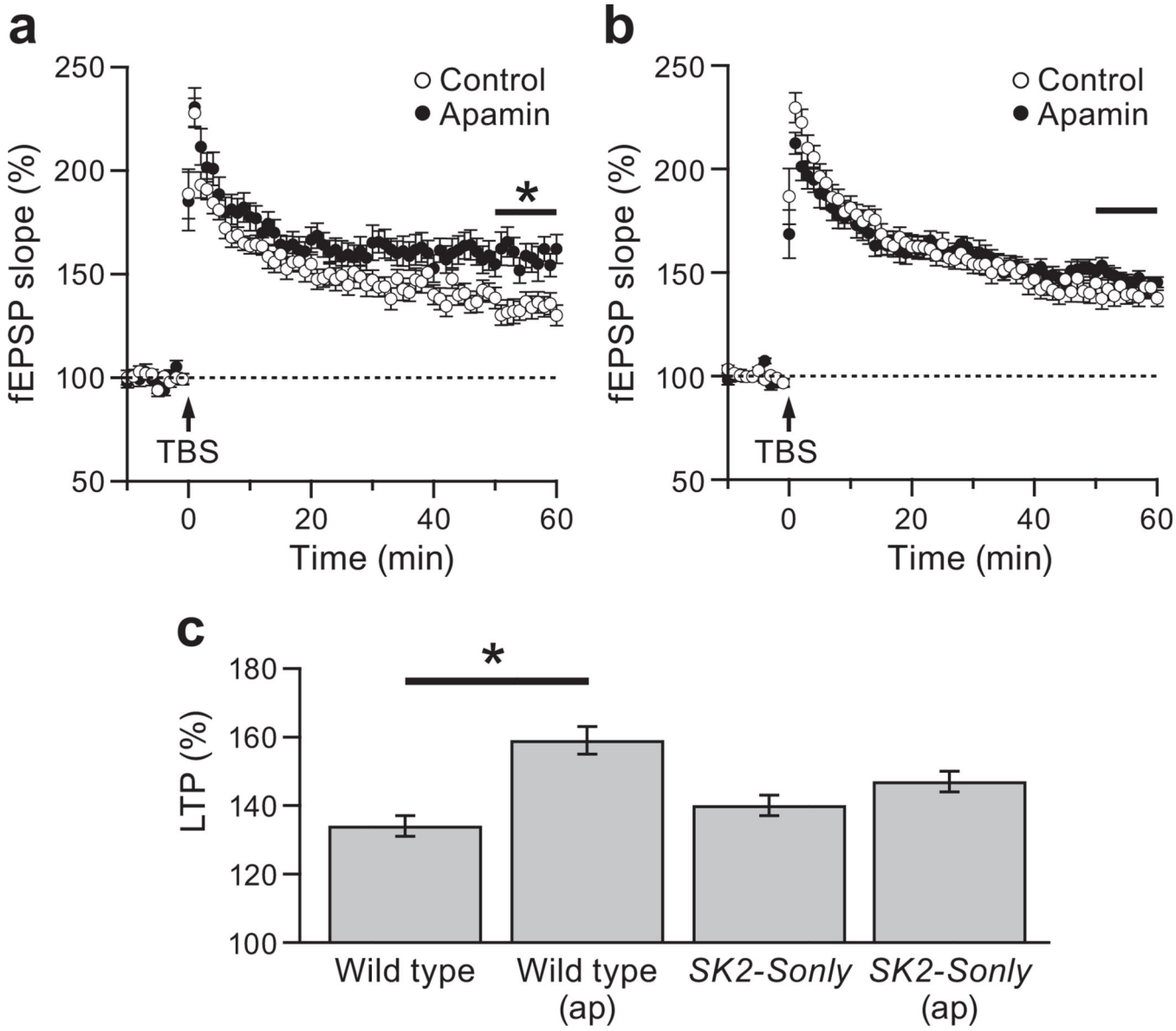

Figure 6. SK channel activity affects LTP in wild type but not *SK2-Sonly* mice

Field potentials were recorded from the CA1 region of hippocampal slices. (**a**) In wild type stimulation of Schaffer collateral axons induced more LTP in the presence of apamin (filled circles) than in control bath solution (open circles); (**b**): LTP was not different with (filled circles) or without (open circles) apamin application in *SK2-Sonly* slices. LTP was measured 50–60 min after stimulation (black bars). (**c**) Summary plot of LTP from the indicated groups. Error bars indicate s.e.m. *P < 0.05.

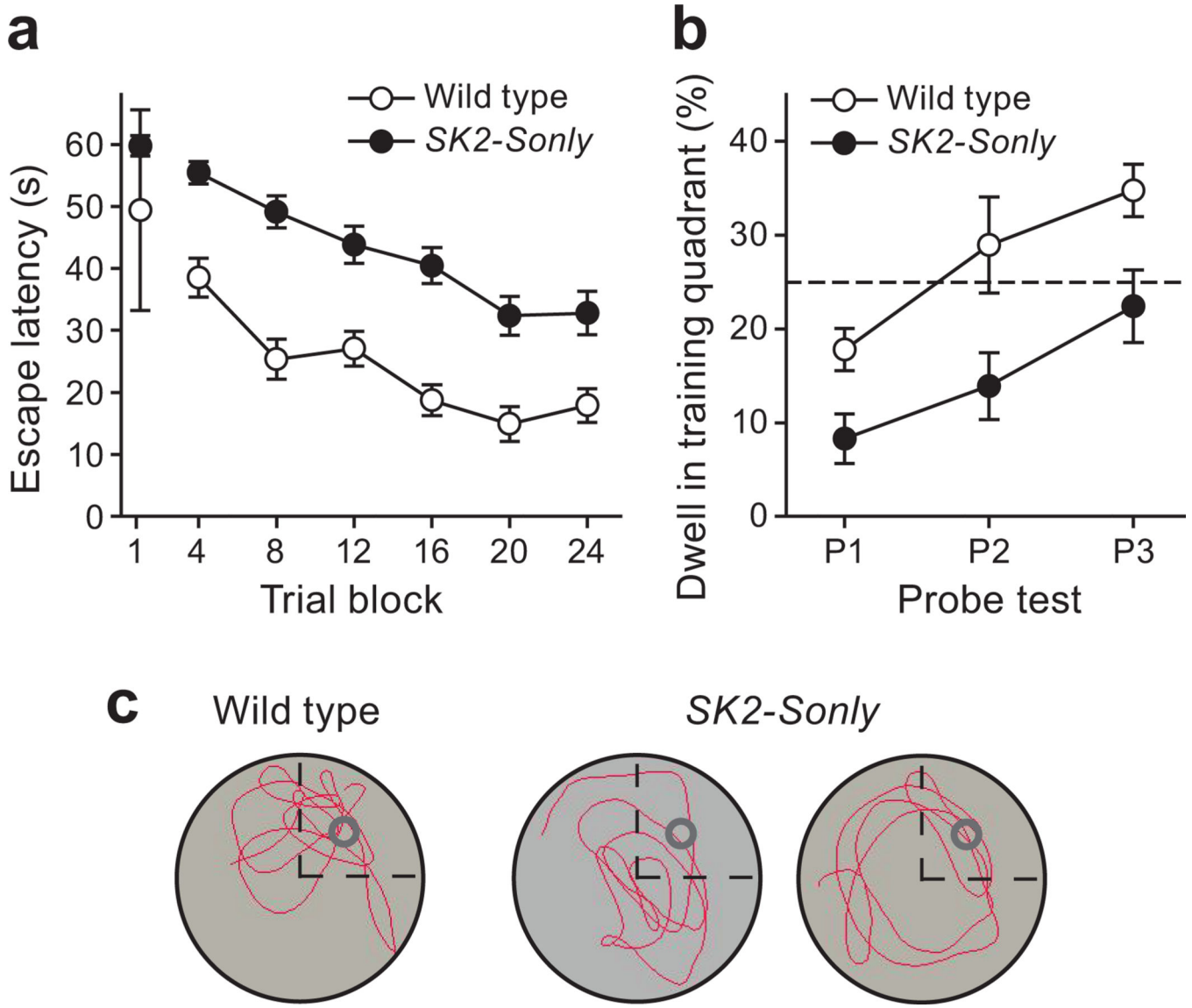

Figure 7. Spatial memory is impaired in *SK2-Sonly* mice

(**a**) The mean latency to escape on to the hidden platform was significantly different between wild type (open circles) and *SK2-Sonly* mice (filled circles). There was no difference between genotypes in mean latency on Trial 1 indicating that both groups exhibited nearly equivalent performance at the start of training. (**b**) The mean % dwell in the correct quadrant of the pool during the probe test of spatial memory retention imposed after the 4th (P1), 12th (P2) and the 20th training trial (P3). The dashed line indicates chance performance. The *SK2-Sonly* mice (filled circles), but not wild type (open circles) failed to exhibit a significant preference for searching in the correct quadrant of the pool. (**c**) Representative paths taken by a wild type mouse (left trace) and two *SK2-Sonly* mice (center and right traces) during the P3 probe test. The path of the WT mouse is direct to training quadrant and then characterized by repetitive passes through the precise location of the pool

where the platform was placed during training (gray open circle). Note that the paths of the *SK2-Sonly* mice are much less accurate and more circuitous than that of the wild type mice.